ACS Medicinal Chemistry Letters

Letter

pubs.acs.org/acsmedchemlett

# Designed Trpzip-3 β-Hairpin Inhibits Amyloid Formation in Two Different Amyloid Systems

Gene Hopping,[†] Jackson Kellock,[†] Byron Caughey,[‡] and Valerie Daggett*,[†]

[†]Department of Bioengineering, University of Washington, Seattle, Washington 98195, United States

[‡]Laboratory of Persistent Viral Diseases, Rocky Mountain Laboratories, National Institute of Allergy and Infectious Diseases, National Institutes of Health, Hamilton, Montana 59840, United States

Supporting Information

**ABSTRACT:** The trpzip peptides are small, monomeric, and extremely stable β-hairpins that have become valuable tools for studying protein folding. Here, we show that trpzip-3 inhibits aggregation in two very different amyloid systems: transthyretin and Aβ(1−42). Interestingly, Trp → Leu mutations renders the peptide ineffective against transthyretin, but Aβ inhibition remains. Computational docking was used to predict the interactions between trpzip-3 and transthyretin, suggesting that inhibition occurs via binding to the outer region of the thyroxine-binding site, which is supported by dye displacement experiments.

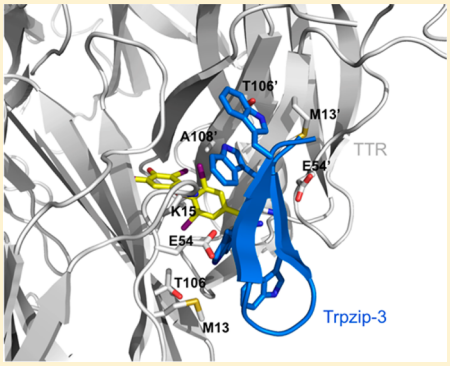


**KEYWORDS:** *Alzheimer's disease, Trpzip, transthyretin, ANS fluorescence, computational docking*

Amyloid disease is characterized by the aggregation of normally soluble peptides and proteins, ultimately resulting in mature fibrils rich in β-sheet structure. The consensus view is that it is the soluble-oligomeric form of these proteins that is the most toxic, while fibrils are relatively inert.[1−4] One popular strategy for combatting this aggregation is the stabilization of the native, low molecular weight structures of these peptides and proteins. Two particularly well-studied amyloid systems are transthyretin (TTR) and the amyloid β-peptide (Aβ).

TTR is a homotetramer consisting of 127 residue monomers with an IgG-like fold in a dimer of dimers arrangement. TTR is a secondary carrier of the thyroid hormone thyroxine in plasma, and it has two binding sites at the dimer−dimer interface. Familial amyloid polyneuropathy (FAP) and senile systemic amyloidosis (SSA) are two diseases caused by tetramer dissociation, partial unfolding, and aggregation of the monomers. Whereas FAP is due to point mutations, SSA is sporadic and present to varying degrees in much of the elderly population.[5] In both cases, tetramer destabilization and partial unfolding of the monomer can lead to aggregation and formation of amyloid fibrils.[6] Tetramer stabilization is a strategy that has been used successfully to reduce TTR aggregation. The endogenous ligand thyroxine, and other polyaromatic molecules including diflunisal,[7] curcumin,[8] and tafamidis[9] stabilize the tetrameric form of TTR and prevent aggregation. Tafamidis (trade name Vyndaquel) is currently in phase II/III clinical trials and has been approved by the European Medicines Agency in 2011 for treatment of FAP.[10] In contrast to TTR, Aβ is a small peptide, and it is relatively unstructured in solution. However, like TTR, it undergoes a conformational change and aggregates; Aβ is the primary proteinaceous component of plaques associated with Alzheimer's Disease. The inhibition of Aβ by peptides containing β-structure is well documented.[11−13] However, to our knowledge there are no accounts of the inhibition of TTR aggregation by peptides. Interestingly a recent account suggested that β-amyloid binds to TTR; however, it appears that the interaction occurs after tetramer dissociation.[14]

We are interested in the development of broad-spectrum inhibitors of amyloid formation. The trpzip peptides are among the smallest β-hairpin peptides known to fold spontaneously without the use of disulfide-bonds or metal ions.[15] The four tryptophan residues are located at every other position in the sheets, resulting in all Trp residues falling on the same face in the folded hairpin. The small size and stability of the trpzip peptide make it an ideal scaffold for peptide inhibitor studies.

Here, we describe investigations of two trpzip peptides to assess their ability to inhibit aggregation in two different amyloid systems: TTR and Aβ. In particular, we focused on trpzip-3 (TZ) and a W → L mutant, where all four Trp residues were replaced with Leu (L4-TZ, or leuzip) (Figure 1A). We chose the W → L mutation to allow us to discern whether any inhibitory properties were due to the trpzip fold specifically, i.e.,

**Received:** December 26, 2012
**Accepted:** August 1, 2013
**Published:** August 1, 2013

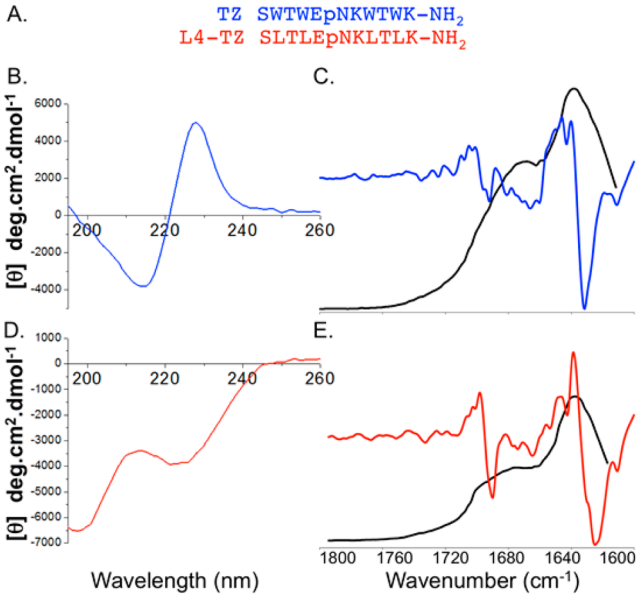


**Figure 1.** Structural characterization of peptides. (A) Primary sequence of TZ and L4-TZ. (B) CD spectrum of TZ showing strong exciton coupling of tryptophan residues centered around 220 nm. (C) FTIR spectrum confirms $\beta$-sheet structure of TZ with a minimum at 1630 $cm^{-1}$. (D) CD spectrum of L4-TZ displaying minima at 220 and 198 nm. (E) FTIR spectrum of L4-TZ, which displays a minimum at 1625 $cm^{-1}$.

the $\beta$-hairpin structure, or interactions with the Trp residues. It has been demonstrated that the contribution of cross-strand interactions between two Leu residues in a similar system, while stabilizing, was much weaker ($\Delta\Delta G$ + 1.25 kcal $mol^{-1}$ when compared to the interaction between two Trp residues).[16] Consequently, we anticipated that the L4-TZ hairpin would remain intact, but possibly be destabilized relative to TZ.

To verify that both peptides formed $\beta$-structures and to ensure that the W to L mutations were well tolerated, we evaluated the global structures of the peptides using circular dichroism (CD) and Fourier transform-infrared (FTIR) spectroscopies (Figure 1). Consistent with previous results, the CD spectrum of TZ shows a strong exciton coupling between the Trp residues, manifesting as a Cotton effect centered at 221 nm (Figure 1B).[15] The FTIR spectrum of TZ shows a strong absorbance at 1630 $cm^{-1}$, consistent with $\beta$-sheet structure[17] (Figure 1C). L4-TZ displays two negative bands in the CD spectrum, centered at 223 and 198 nm, indicative of $\beta$-sheet and random coil content, respectively (Figure 1D). The FTIR spectrum confirms $\beta$-sheet, with a strong absorbance at 1630−1625 $cm^{-1}$ (Figure 1E). Interestingly, the FTIR spectrum suggests more ordered $\beta$-structure than might be expected based on the CD,[17] which may result from analyzing the peptide as a dried film. Analytical size exclusion chromatography of a sample of L4-TZ that had been in solution for 1 week showed it to be monomeric (Figure S1, Supporting Information). L4-TZ unfolded irreversibly, as probed via variable temperature CD spectroscopy (Figure S2, Supporting Information), in contrast to TZ, which displays reversible and highly cooperative unfolding.[18] Taken together, these results indicate that the W → L mutation TZ variant exists as a monomeric, soluble $\beta$-hairpin in solution, although it is somewhat less structured than TZ in solution.

To evaluate the antiamyloidogenic properties of the designs, a large excess of TZ or L4-TZ was coincubated with TTR or A$\beta$, and aggregation was monitored via Congo red binding or ThT fluorescence, respectively, relative to uninhibited aggregation (Figure 2). TTR and A$\beta$ spontaneously aggregate

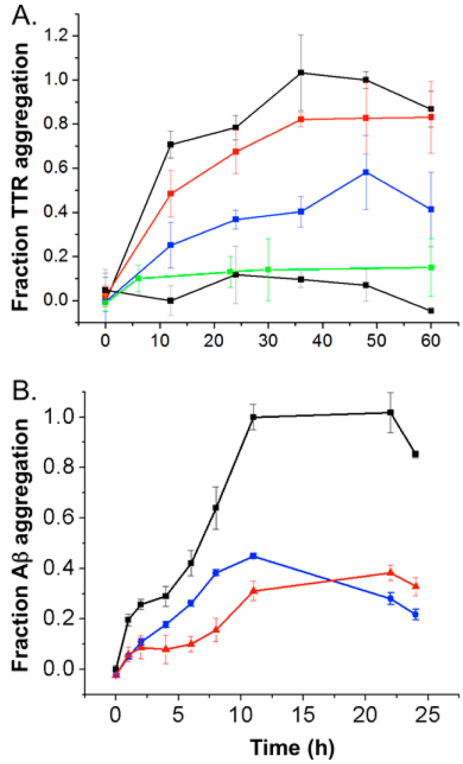


**Figure 2.** Inhibition of amyloid formation. (A) Inhibition of TTR aggregation. TTR was allowed to aggregate at pH 4.5 in the absence of peptide (black) or with 20 mol equiv of TZ (blue) or L4-TZ (red). To determine maximal inhibition, TTR was incubated at neutral pH to prevent aggregation (gray). Results for the addition of 2 equivalents of the small molecule diflunisal is shown for reference (green). (B) Inhibition of A$\beta$ aggregation. A$\beta$ was allowed to aggregate at neutral pH in the absence of inhibitor (black) or presence of 10 mol equiv of TZ (blue) or L4-TZ (red).

at low pH and neutral pH, respectively. We were unable to use ThT to monitor fibril formation in the TTR assay, as the addition of ThT to freshly dissolved and filtered TTR gives high background fluorescence, which obscures any increase upon fibril formation, as has been documented by others.[19] A 20-fold excess of peptide was incubated with TTR, and 10-fold excess of peptide was incubated with A$\beta$. TTR aggregation was evaluated at the peak Congo red value (36 h). TZ inhibited aggregation by 60% when coincubated with TTR. In contrast, no inhibition was observed for L4-TZ under these conditions. For comparison, 2 equivalents of the small molecule inhibitor diflunisal resulted in greater than 90% inhibition of aggregation under these conditions (Figure 2A). Congo red binds multiple species during the aggregation process, not just fibrils. We therefore performed AFM and confirmed that fibrils were present in both the uninhibited TTR sample and the TTR + L4-TZ sample. In contrast, there was little fibril formation in the TTR + TZ sample, supporting the ability of TZ to inhibit fibril formation (Figure S3, Supporting Information). Lowering the concentration of TZ from 20 to 10 equivalents produced no change in the inhibition; however, only 16% and 8% inhibition


dx.doi.org/10.1021/ml300478w | ACS Med. Chem. Lett. 2013, 4, 824−828

was observed for 5 and 2 equivalents, respectively (Figure S4, Supporting Information). Interestingly, A$\beta$, however, was inhibited by both peptides. At 12 h, 55% of A$\beta$ aggregation was inhibited by TZ and 69% inhibition was achieved with L4-TZ (Figure 2B).

Both TZ and L4-TZ inhibited A$\beta$ during the early stages of aggregation, which suggests that they are interacting with the monomer versus the soluble aggregates. The inhibition of TTR by only one of the hairpins was interesting given the ability of both to inhibit A$\beta$. Considering both peptides are $\beta$-hairpins, our initial assumption was that the hydrophobic face formed by the four Trp residues of TZ was responsible for TTR inhibition, whereas it was most likely the $\beta$-sheet itself that inhibited A$\beta$. It is well-known that TTR must first dissociate to the monomer before partial unfolding and aggregation can occur,[20] while A$\beta$ aggregates from a relatively unstructured monomer.[21] The interaction between TZ and TTR could occur in one of two ways: with the monomer since tetramer dissociation would provide previously buried hydrophobic surfaces that could interact with TZ; or with the tetramer possibly through the two hydrophobic thyroxine binding sites.

Previous work has shown that the fluorescent dye 8-anilinonaphthalene-1-sulfonate (ANS) binds in the thyroxine binding-sites of TTR, competitively displacing thyroxine.[22] To begin dissecting the mechanism of TZ inhibition of TTR aggregation, we performed an ANS displacement assay to see whether the TZ could displace ANS from TTR tetramers. We first saturated the thyroxine binding sites with ANS, and then attempted to competitively displace the dye with our peptide. In good agreement with previous experiments, we found titration of tetrameric TTR with ANS resulted in a peak fluorescence value at approximately 2 equivalents of ANS for every TTR tetramer, indicating saturation of the thyroxine binding site[22] (Figure S5, Supporting Information). Further addition of TTR resulted in a decrease in the fluorescence signal, presumably due to the increasing absorbance of unbound dye. Next we incubated increasing concentrations of peptide in a solution of 1 $\mu$M tetrameric TTR and 2 $\mu$M ANS. (Figure 3) Complete loss of fluorescence occurred after the addition of 13.5 $\mu$M TZ, returning fluorescence to levels observed in the absence of TTR, indicating that all the ANS was displaced from the TTR binding site. Similar titration of L4-TZ failed to influence the fluorescence, indicating that L4-TZ was not interacting with the thyroxine-binding site. Maintenance of the tetrameric structure of TTR was confirmed at high concentrations of TZ by size exclusion chromatography, supporting our hypothesis that TZ is interacting with the tetramer and not stabilizing TTR as monomers or dimers (Figure S6, Supporting Information; note also the agreement between the TTR-TZ and TTR-diflunisal traces).

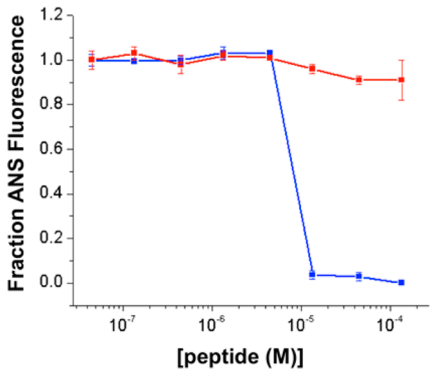


**Figure 3.** TZ displaces ANS fluorescence. Increasing concentrations of TZ (blue) or L4-TZ (red) were incubated with a solution containing 1 $\mu$M TTR and 2 $\mu$M ANS, and changes in ANS fluorescence were observed. Addition of 13.5 $\mu$M TZ returned fluorescence levels to those observed in the absence of TTR, indicating displacement of ANS from the tetramer. Similar addition of up to 135 $\mu$M L4-TZ failed to affect the fluorescence.

Each TTR tetramer contains two thyroxine-binding sites, located in channels formed at the dimer−dimer interface. Three cavities are defined by symmetric pairs of residues from each monomer that line the channel. The arrangement of the hydrophobic portions of the side chains create small pockets, named the halogen binding pockets that accommodate the iodine atoms of thyroxine.[23] The innermost cavity consists of residues Ala 109/109′, Leu 110/110′, Ser 117/117′, and Thr 119/119′. The middle cavity consists of residues Lys 15/15′, Leu 17/17′, Ala 109/109′, and Leu 110/110′. The outermost pocket, closest to the surface of the molecule, is defined by residues Met 13/13′, Lys 15/15′, Thr 106/106′, and Ala 108/108′.[24] To rationalize the displacement of ANS by TZ, we performed computational docking using HADDOCK.[25,26]

For the HADDOCK calculations, we defined "active" residues in the TTR tetramer as residues Lys 15/15′ and Ala 108/108′ due to their location in the outer binding pocket and experimentally observed interaction with thyroxine in the crystal structure.[24] The four Trp residues of TZ were chosen as active residues due to loss of inhibition of TTR aggregation but maintenance of $\beta$-hairpin structure upon mutation to Leu. From the pool of 200 structures, the two top scoring clusters contained 108 and 82 structures, respectively, which accounted for 95% of all models that proceeded to the water refinement stage. In both cases, the peptide is oriented in the thyroxine binding site with the strands parallel to strand A and A′ of TTR (Figure 4A); however, the structures in cluster 2 are rotated 180 degrees with respect to the structures in cluster 1 (Figure 4B). In both clusters, the Trp-containing faces are oriented toward the protein, burying the hydrophobicity of the side-chains and forming contacts with both monomers. While the TZ molecule is too big to be accommodated entirely within the thyroxine binding site, the Trp residues enter the binding site far enough to form hydrophobic interactions with all outer binding pocket residues with the exception of Ala108/108′. Additional contacts include Ser 52/52′, His 56/56′, and Val 121/121′.

To further investigate the 180° rotation of the docked ensembles, we performed molecular dynamics (MD) simulations of TZ in order to gain insight into the side chain dynamics of the Trp residues. We found that the $\chi_1$ rotamer preference of the NMR structure was held throughout a 100 ns simulation, as would be expected to maintain the trpzip fold.[15] The $\chi_1$ rotamers for TZ populated were gauche- for residues 2 and 9 ($-77.04 \pm 19.86°$ and $-71.23 \pm 13.04°$) and trans for residues 4 and 11 ($179.62 \pm 10.56°$ and $-177.93 \pm 12.77°$). When visualized in their 3D arrangement in the hairpin, Trp 4 and Trp 9 are in the center of the molecule, flanked by Trp 2 and Trp 11, creating a 2-fold axis of symmetry with respect to the side chains alone. Therefore, the two ensembles populated during the docking represent similar solutions. Many contacts between TZ ensemble 1 (Figure 5A) and monomer A are repeated between ensemble 2 (Figure 5B) and monomer A′.


dx.doi.org/10.1021/ml300478w | ACS Med. Chem. Lett. 2013, 4, 824−828

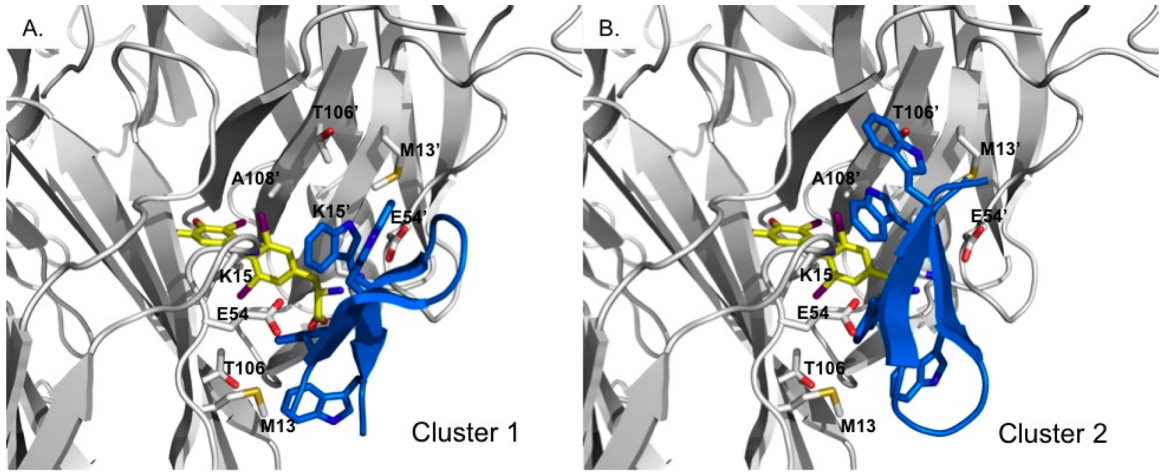


**Figure 4.** Top docking results are both located in the outer region of the thyroxine binding site. Each ensemble is represented by the lowest energy structures (blue). (A) Ensemble 1. TZ backbone is represented as cartoon, with the tryptophan side chains represented as sticks. (B) Ensemble 2. The backbone, while positioned in a similar region of the thyroxine binding site, is oriented 180° with respect to ensemble 1. In both panels, the position of thyroxine (yellow) in the crystal structure is shown.

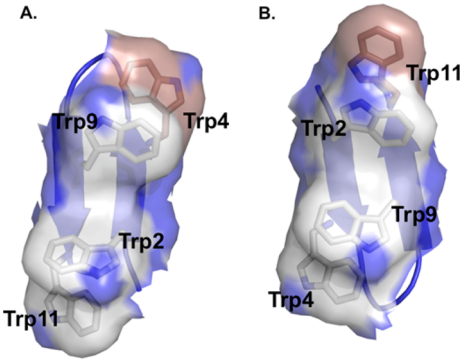


**Figure 5.** Surface representation of tryptophan residues of the top docked results. Comparison of tryptophan side chain positions reveals a common hydrophobic surface formed by (A) Trp residues 2, 9, and 11 in ensemble 1 and (B) residues 2, 4, and 9 in ensemble 2. The tryptophan residues not forming part of the surface are colored brown. Each structure is rotated 180° from each other, revealing similar surfaces despite backbone orientation.

The interaction of TZ with the majority of the residues in the outer binding pocket of TTR, while weak, appears to be sufficient to displace ANS. The displacement of ANS confirms interaction with the tetrameric protein, as once the tetramer dissociates the thyroxine binding site no longer exists. Taken together, the interaction between TZ and tetrameric TTR and subsequent inhibition of amyloid formation indicate that TZ is stabilizing TTR in the tetrameric form. This stabilization prevents dissociation to the monomer from which aggregation occurs. This mechanism has been demonstrated with many small molecule inhibitors, including tafamidis and the diflusinal control presented here.[27,28]

Crystal structures of TTR with both tafamidis and diflunisal bound are available (3TCT and 3D2T, respectively).[29,30] Both make contact with all three cavities within the binding channel. The 3,5-dichloro groups of tafamidis and the 2,4-difluoro groups on diflunisal are buried in the innermost core, making contact with Ser 117, Thr 119, and Leu 110. The remainder of the molecules makes contact with all residues of the middle cavity. The carboxylate groups of tafamidis point toward the opening of the cavity, and because of the pseudo axis of symmetry, alternate conformations interact with both Lys 15 and Glu 54 via water bridges. Diflunisal is shorter and does not extend as far as tafamidis and only makes contact with Lys 15. In contrast, TZ lies parallel to the binding channel, with Trp residues oriented toward the channel. The TZ residues only interact with the outer pocket, except for Ala 108, and instead make additional outer surface contacts with Ser 52, His 56, and Val 121.

We have shown novel amyloid inhibitory properties of the trpzip-3 (TZ) peptide against A$\beta$ and TTR. Through dye displacement and computational docking, we predict that inhibition of TTR aggregation occurs via interaction with the tetramer, whereby the Trp-containing face of TZ interacts with the outer residues of both faces of the thyroxine binding site. The small size and stability of the trpzip scaffold makes it a good template for future peptide-based drug designs aimed at improving the affinity.

## ■ ASSOCIATED CONTENT

### Ⓢ Supporting Information

Supplementary Figures 1−6 and full experimental methods. This material is available free of charge via the Internet at http://pubs.acs.org.

## ■ AUTHOR INFORMATION

### Corresponding Author

*(V.D.) E-mail: daggett@u.washington.edu. Phone: (206) 685-1510.

### Author Contributions

G.H. designed and performed experiments, analyzed data, and wrote the paper. J.K. performed experiments. B.C. designed and performed experiments. V.D. designed experiments, analyzed data, and wrote the paper. The manuscript was written through contributions of all authors.

### Funding

This work was funded by the W. H. Coulter Foundation Translational Research Partnership Program (to V.D.), a grant from the National Science Foundation (CBET-0966977 to V.D.), the Coins for Alzheimer's Research Trust (to V.D.), and the Intramural Research Program of the NIAID (to B.C.).

### Notes

The authors declare no competing financial interest.

## ■ ACKNOWLEDGMENTS

We thank Drs. David Baker, Pat Stayton, Ceci Giachelli, and Roland Strong for generous use of equipment. We thank Drs. Colin Correnti and Peter Rupert for assistance with SEC and Dr. Clare Towse for review of the manuscript. Part of this work was conducted at the University of Washington NanoTech User Facility, a member of the NSF National Nanotechnology Infrastructure Network (NNIN).

## ■ ABBREVIATIONS

TZ, trpzip-3; L4-TZ, mutant TZ in which the 4 Trp residues are substituted by Leu; TTR, transthyretin, A$\beta$, $\beta$-amyloid (1−42); ANS, 8-anilinonaphthalene-1-sulfonate

## ■ REFERENCES

(1) Bucciantini, M.; Giannoni, E.; Chiti, F.; Baroni, F.; Formigli, L.; Zurdo, J.; Taddei, N.; Ramponi, G.; Dobson, C. M.; Stefani, M. Inherent toxicity of aggregates implies a common mechanism for protein misfolding diseases. *Nature* **2002**, *416*, 507−511.

(2) Hardy, J.; Selkoe, D. J. The amyloid hypothesis of Alzheimer's disease: progress and problems on the road to therapeutics. *Science* **2002**, *297*, 353−356.

(3) Tomic, J. L.; Pensalfini, A.; Head, E.; Glabe, C. G. Soluble fibrillar oligomer levels are elevated in Alzheimer's disease brain and correlate with cognitive dysfunction. *Neurobiol. Dis.* **2009**, *35*, 352−358.

(4) Xue, W.-F.; Hellewell, A. L.; Gosal, W. S.; Homans, S. W.; Hewitt, E. W.; Radford, S. E. Fibril fragmentation enhances amyloid cytotoxicity. *J. Biol. Chem.* **2009**, *284*, 34272−34282.

(5) Tanskanen, M.; Peuralinna, T.; Polvikoski, T.; Notkola, I.-L.; Sulkava, R.; Hardy, J.; Singleton, A.; Kiuru-Enari, S.; Paetau, A.; Tienari, P. J.; Myllykangas, L. Senile systemic amyloidosis affects 25% of the very aged and associates with genetic variation in alpha2-macroglobulin and tau: a population-based autopsy study. *Ann. Med.* **2008**, *40*, 232−239.

(6) Hurshman, A. R.; White, J. T.; Powers, E. T.; Kelly, J. W. Transthyretin aggregation under partially denaturing conditions is a downhill polymerization. *Biochemistry* **2004**, *43*, 7365−7381.

(7) Adamski-Werner, S. L.; Palaninathan, S. K.; Sacchettini, J. C.; Kelly, J. W. Diflunisal analogues stabilize the native state of transthyretin. Potent inhibition of amyloidogenesis. *J. Med. Chem.* **2004**, *47*, 355−374.

(8) Pullakhandam, R.; Srinivas, P. N. B. S.; Nair, M. K.; Reddy, G. B. Binding and stabilization of transthyretin by curcumin. *Arch. Biochem. Biophys.* **2009**, *485*, 115−119.

(9) Bulawa, C. E.; Connelly, S.; Devit, M.; Wang, L.; Weigel, C.; Fleming, J. A.; Packman, J.; Powers, E. T.; Wiseman, R. L.; Foss, T. R.; Wilson, I. A.; Kelly, J. W.; Labaudinière, R. Tafamidis, a potent and selective transthyretin kinetic stabilizer that inhibits the amyloid cascade. *Proc. Natl. Acad. Sci. U.S.A.* **2012**, *109*, 9629−9634.

(10) de Carvalho, M. Is it better than it seems or just good enough? The tafamidis saga. *Muscle Nerve* **2012**, *46*, 14−14.

(11) Yamin, G.; Ruchala, P.; Teplow, D. B. A peptide hairpin inhibitor of amyloid $\beta$-protein oligomerization and fibrillogenesis. *Biochemistry* **2009**, *48*, 11329−11331.

(12) Huggins, K. N. L.; Bisaglia, M.; Bubacco, L.; Tatarek-Nossol, M.; Kapurniotu, A.; Andersen, N. H. Designed hairpin peptides interfere with amyloidogenesis pathways: fibril formation and cytotoxicity inhibition, interception of the preamyloid state. *Biochemistry* **2011**, *50*, 8202−8212.

(13) Smith, T. J.; Stains, C. I.; Meyer, S. C.; Ghosh, I. Inhibition of beta-amyloid fibrillization by directed evolution of a beta-sheet presenting miniature protein. *J. Am. Chem. Soc.* **2006**, *128*, 14456−14457.

(14) Du, J.; Cho, P. Y.; Yang, D. T.; Murphy, R. M. Identification of beta-amyloid-binding sites on transthyretin. *Protein Eng., Des. Sel.* **2012**, *25*, 337−345.

(15) Cochran, A. G.; Skelton, N. J.; Starovasnik, M. A. Tryptophan zippers: stable, monomeric beta -hairpins. *Proc. Natl. Acad. Sci. U.S.A.* **2001**, *98*, 5578−5583.

(16) Russell, S. J.; Cochran, A. G. Designing stable beta-hairpins: Energetic contributions from cross-strand residues. *J. Am. Chem. Soc.* **2000**, *122*, 12600−12601.

(17) Barth, A.; Zscherp, C. What vibrations tell about proteins. *Q. Rev. Biophys.* **2002**, *35*, 369−430.

(18) Cochran, A. G.; Tong, R. T.; Starovasnik, M. A.; Park, E. J.; McDowell, R. S.; Theaker, J. E.; Skelton, N. J. A minimal peptide scaffold for $\beta$-turn display: Optimizing a strand position in disulfide-cyclized $\beta$-hairpins. *J. Am. Chem. Soc.* **2001**, *123*, 625−632.

(19) Sinha, S.; Lopes, D. H. J.; Du, Z.; Pang, E. S.; Shanmugam, A.; Lomakin, A.; Talbiersky, P.; Tennstaedt, A.; McDaniel, K.; Bakshi, R.; Kuo, P.-Y.; Ehrmann, M.; Benedek, G. B.; Loo, J. A.; Klärner, F.-G.; Schrader, T.; Wang, C.; Bitan, G. Lysine-specific molecular tweezers are broad-spectrum inhibitors of assembly and toxicity of amyloid proteins. *J. Am. Chem. Soc.* **2011**, *133*, 16958−16969.

(20) Foss, T. R.; Wiseman, R. L.; Kelly, J. W. The pathway by which the tetrameric protein transthyretin dissociates. *Biochemistry* **2005**, *44*, 15525−15533.

(21) Maji, S. K.; Amsden, J. J.; Rothschild, K. J.; Condron, M. M.; Teplow, D. B. Conformational dynamics of amyloid $\beta$-protein assembly probed using intrinsic fluorescence. *Biochemistry* **2005**, *44*, 13365−13376.

(22) Cheng, S.; Pages, R.; Saroff, H.; Edelhoch, H. Analysis of thyroid hormone binding to human serum prealbumin by 8-anilinonaphthalene-1-sulfonate fluorescence. *Biochemistry* **1977**, *16*, 3707−3713.

(23) Connelly, S.; Choi, S.; Johnson, S. M.; Kelly, J. W.; Wilson, I. A. Structure-based design of kinetic stabilizers that ameliorate the transthyretin amyloidoses. *Curr. Opin. Struct. Biol.* **2010**, *20*, 54−62.

(24) Wojtczak, A.; Cody, V.; Luft, J. R.; Pangborn, W. Structures of human transthyretin complexed with thyroxine at 2.0 A resolution and 3″,5″-dinitro-*N*-acetyl-L-thyronine at 2.2 Å resolution. *Acta Crystallogr., Sect. D: Biol. Crystallogr.* **1996**, *D52*, 758−765.

(25) Dominguez, C.; Boelens, R.; Bonvin, A. M. J. J. HADDOCK: a protein−protein docking approach based on biochemical or biophysical information. *J. Am. Chem. Soc.* **2003**, *125*, 1731−1737.

(26) de Vries, S. J.; van Dijk, M.; Bonvin, A. M. J. J. The HADDOCK web server for data-driven biomolecular docking. *Nat. Protoc.* **2010**, *5*, 883−897.

(27) Miroy, G. J.; Lai, Z.; Lashuel, H. A.; Peterson, S. A.; Strang, C.; Kelly, J. W. Inhibiting transthyretin amyloid fibril formation via protein stabilization. *Proc. Natl. Acad. Sci. U.S.A.* **1996**, *93*, 15051−15056.

(28) Choi, S.; Reixach, N.; Connelly, S.; Johnson, S. M.; Wilson, I. A.; Kelly, J. W. A substructure combination strategy to create potent and selective transthyretin kinetic stabilizers that prevent amyloidogenesis and cytotoxicity. *J. Am. Chem. Soc.* **2010**, *132*, 1359−1370.

(29) Bulawa, C. E.; Connelly, S.; Devit, M.; Wang, L.; Weigel, C.; Fleming, J. A.; Packman, J.; Powers, E. T.; Wiseman, R. L.; Foss, T. R.; Wilson, I. A.; Kelly, J. W.; Labaudiniere, R. Tafamidis, a potent and selective transthyretin kinetic stabilizer that inhibits the amyloid cascade. *Proc. Natl. Acad. Sci. U.S.A.* **2012**, *109*, 9629−9634.

(30) Adamski-Werner, S. L.; Palaninathan, S. K.; Sacchettini, J. D.; Kelly, J. W. Diflunisal analogues stabilize the native state of transthyretin. Potent inhibition of amyloidogenesis. *J. Med. Chem.* **2004**, *47*, 355−374.